



Acoustic Emissions versus Pressure Stimulated Currents during bending of restored marble epistyles: Preliminary results

Stavros K. Kourkoulis, Ioanna Dakanali, Ermioni D. Pasiou

National Technical University of Athens,

School of Applied Mathematical and Physical Sciences, Department of Mechanics,

5 Heroes of Polytechnion Avenue, Theocaris Bld., Zografou Campus, 157 73 Athens, Greece

stakour@central.ntua.gr

Ilias Stavrakas, Dimos Triantis

Technological Educational Institution of Athens,

Department of Electronics, Laboratory of Electronic Devices and Materials,

Agion Spiridonos Street, 122 10, Athens, Greece

ABSTRACT. The efficiency of two modern sensing techniques, namely the “Acoustic Emissions” and the “Pressure Stimulated Currents” ones, when they are used as Continuous Structural Health Monitoring tools, is assessed experimentally. The protocol includes multi-point bending of an accurate copy of a fractured marble epistyle of the Parthenon’s Temple on the Acropolis of Athens, under a scale of 1:3. The integrity of the epistyle is restored with three pairs of bolted titanium bars, according to the pioneering technique developed by the scientists of the “Committee for the Conservation of the Acropolis Monuments”. The data provided by the above techniques are considered in juxtaposition to each other and also in comparison to data provided by the “Digital Image Correlation” technique. It is concluded that, at least from a qualitative point of view, the data of all three techniques are in good mutual agreement. Combined exploitation of the various sets of experimental data enlightens interesting aspects concerning the succession of failure mechanisms activated during the loading procedure, revealing the critical role of the internal interfaces characterizing the restored epistyle. Moreover it is definitely indicated that both the “Acoustic Emissions” and the “Pressure Stimulated Currents” techniques provide clear signs of upcoming failure well before macroscopically visible damages are detected at the external surface of the specimen.

KEYWORDS. Acoustic Emissions; Pressure Stimulated Currents; Digital Image Correlation; Marble Monuments; Restoration/Conservation; Continuous Structural Health Monitoring.



Citation: Kourkoulis, S.K., Dakanali, I., Pasiou, E.D., Stavrakas, I., Triantis, D., Acoustic Emissions versus Pressure Stimulated Currents during bending of restored marble epistyles: Preliminary results, *Frattura ed Integrità Strutturale*, 41 (2017) 536-551.

Received: 30.04.2017

Accepted: 31.05.2017

Published: 01.07.2017

Copyright: © 2017 This is an open access article under the terms of the CC-BY 4.0, which permits unrestricted use, distribution, and reproduction in any medium, provided the original author and source are credited.



INTRODUCTION

Continuous structural health monitoring (CSHM) is perhaps the most effective tool in hands of structural engineers, in the direction of timely detecting accumulation of damage in structures of any kind. It offers, thus, the time interval, which is necessary in order for proper measures to be undertaken, preventing further damage accumulation that can lead to catastrophic failures. The topic is in the cutting edge of scientific research worldwide, since according to the ancient Greek physician and philosopher Hippocrates “*prevention is better than cure*”. Nowadays, research is focused on the development and practical implementation of new ideas (both in the hardware and the software level) for CSHM, which are flexible, user-friendly and also effective from the financial point of view.

The field of restoration and conservation of cultural heritage monuments is among the ones for which CSHM is a “*conditio sine qua non*” for an intervention to be considered successful and completed. In the specific field, however, there are quite a few additional requirements (mainly of aesthetic origin) that do not permit the use of traditional sensing techniques. For example, the size of the devices used as sensors should be very small in order to avoid distorting the beauty and harmony of the external appearance of the monuments. Along the same lines, attaching the sensing devices to the structural members should be implemented very carefully in order to avoid harming the integrity of the member’s external surface.

Besides the as above practical complexities, additional problems must be solved in case of CSHM of cultural heritage monuments, related to the proper interpretation of the data recorded by the sensing devices which are attached on restored structural elements. Indeed, in quite a few cases, restoration of damaged or fractured members is achieved with the aid of metallic reinforcing elements and suitable adhesive materials. As a result, a three-material complex with material interfaces is created, the constituent elements of which are usually of completely different mechanical behaviour and response to any kind of external stimuli.

A typical example of such a restoration approach is the technique adopted nowadays for restoring the integrity of structural elements of the monuments of the Sacred Hill of the Acropolis of Athens. These monuments, which constitute a unique complex of buildings, including the Parthenon, Propylaia, Erechtheion and the temple of Athena Nike, were built by the ancient Greeks during the 5th century B.C. using almost exclusively Pentelic marble. Nowadays, their historical and aesthetic magnificence is recognized worldwide and they are listed among the masterpieces of classical western civilization. The main restorative intervention on the Athenian Acropolis monuments was directed by N. Balanos in 1885. The interventions were of a major scale and their basic principle was that all fragments of structural elements, spread around the monument, should be re-positioned on the monument and the addition of elements made of new material should be as limited as possible. From this moment on, the term “anastylosis” was established as a reconstruction technique whereby ruined monuments are restored using the original architectural elements to the greatest degree possible.

From a purely archeological point of view Balanos’ intervention was successful due to the minimum possible use of new marble, although the use of scattered ancient fragments as ordinary building material has been strongly criticized. Unfortunately from the structural and chemical points of view, the use of metallic reinforcing elements (which were made of steel) without prior verification of their mechanical and physico-chemical compatibility with the ancient material and without taking into account their chemical resistance against air pollution became the source of extensive damage of the monument [1]. In the direction of curing these problems the “Committee for the Conservation of the Acropolis Monuments” (ESMA) was established in 1975 inaugurating a new approach to the restoration of the Acropolis of Athens monuments [1]. The scientific personnel of the committee developed a pioneer technique for the restoration of the structural integrity of the monuments’ structural members, according to which the fractured marble elements are connected by inserting titanium bars into pre-drilled holes. The adhesion between marble and bars is achieved by a proper white cement paste [2, 3]. The aforementioned technique is based on the basic restoration principles, dictated by the “Venice Charter” [4, 5]: Reversibility (if needed, the monument could be brought to its state prior to the intervention), minimization of the interventions to the extent that guarantees protection of the authentic material from further damage (for this reason the number of titanium bars required by the connection’s design, should be the smallest possible) and finally compatibility between the materials used for the restoration and the authentic ones.

The restoration approach described above was assessed a few years ago both experimentally and numerically [6-10]. It has been indicated that, in spite of its efficiency and general acceptance, there are still some open issues that should be further studied, mainly in the direction of reducing the intervention on the authentic building material. In this context an experimental protocol was recently implemented [11, 12], during which accurate copies of fractured epistyles, restored according to the as above procedure, were submitted to multi-point bending in order to simulate the actual loading conditions that will be realized after the epistyle is re-placed in its original position. The main innovation of that study was the simultaneous use of traditional and innovative sensing techniques that permitted pumping data both from the outer surface of the specimens as well as from their interior and especially from the two interfaces (marble-to-cement and cement-to-metal) which

are the areas most suspicious for failure to start. The results were very encouraging, revealing interesting data about the succession of failure mechanisms activated during loading the restored epistyle.

In the present study advantage is taken of the experimental data of that protocol along a different line of thought, namely that of detecting indicators that could play the role of pre-failure warnings. In this direction, the data recorded by the Acoustic Emissions (AE) and the Pressure Stimulated Currents (PSC) techniques are considered in juxtaposition to each other as well as in comparison to the data recorded by the Digital Image Correlation (DIC) technique. It is concluded that the data provided by both the AE and the PSC techniques include clear signs which precede well the upcoming failure of the structure. Taking into account that the AE is already a more or less well established CSHM technique [13-17] (which means that the respective data can be used as a calibration/validation standard) and also the fact that the PSC technique is characterized by very low application cost, it can be concluded that (after proper calibration) the specific technique could be considered as a flexible alternative tool for effective and economically tolerable CSHM, given that its results are here successfully checked against the respective ones of the AE technique.

THE EXPERIMENTAL PROTOCOL AND THE SENSING TECHNIQUES USED

The specimen and the experimental procedure

The experimental procedure is analytically described in ref. [12]. For the convenience of the reader, its main features only are here shortly outlined: An accurate copy of an authentic epistyle of the Parthenon Temple was constructed under a scale 1:3, by experienced technicians of the Parthenon worksite. The epistyle was made of Dionysos marble, the material that is nowadays used, almost exclusively, for the restoration project of the Acropolis monuments, given that the quarries of mount Pentelicon are not accessible, for historic and environmental reasons. The characteristics of Dionysos marble are very close to the respective ones of Pentelic marble from mechanical, geological and physico-chemical points of view [18]. During the construction of the copy every effort was paid for the accurate reproduction of the characteristics of the authentic epistyle especially concerning the orientation of the material layers with respect to the longitudinal axis of the member (and therefore to the direction of the load imposed). It is here recalled that Dionysos and Pentelic marbles are orthotropic materials characterized by three distinct anisotropy axes, although along two of them the mechanical properties are quite close to each other and therefore both materials are usually simulated as transversely isotropic ones [19, 20]. Obviously, in case of bending, optimum load-bearing capacity is achieved when the material layers are normal to the loading line.

The copy of the epistyle was asymmetrically fractured into two fragments, which were restored with the aid of three pairs of bolted titanium bars driven in pre-drilled holes, as it can be clearly seen in Fig.1a. The holes are filled with a suitable cement paste (binder and water without aggregates), which acts both as adhesion layer and also as matching element between the two extremely incompatible basic constituents of the complex (i.e., the extremely brittle marble and the extremely ductile titanium) protecting the authentic building stone. The angle of the fracture plane with respect to the axis of the member was 70°. The specific choice is based on observations of fracture planes of epistyles of the Parthenon Temple and it appears to be the maximum one for which the specific arrangement of reinforcing bars could be applied. The bar's anchoring length

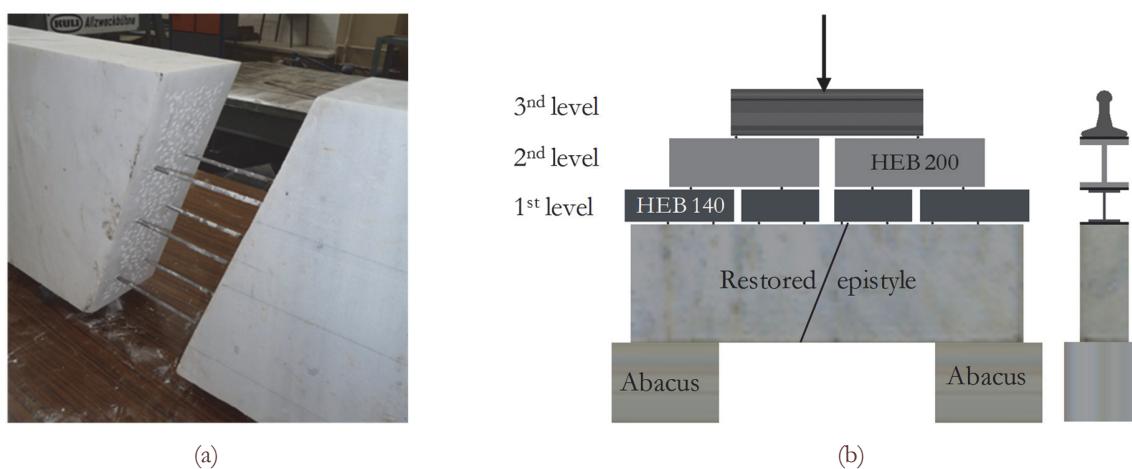


Figure 1: (a) The two fragments of the epistyle's copy during the restoration phase. The three pairs of reinforcing elements are clearly visible; (b) Schematic representation of the multi-point bending loading scheme.

for both fragments was equal to 25 cm, symmetrically with respect to the fracture plane. The surfaces of the fragments that were to come in contact were coated with the same cement paste (used to fill the holes) to ensure optimum matching of the fragments rather than to increase the element's bearing capacity (the tensile strength of the cement paste is negligible). After curing for 28 days the specimen was placed on two marble cubes (simulating the in-situ supporting conditions, i.e. the capitals or abacuses of the Temple) on the platform of a very stiff (capacity 6 MN) servo-hydraulic loading frame. For the load transferred to the epistyle to be as uniformly distributed as possible, a three-level steel construction was placed above the specimen, as it is shown schematically in Fig.1b. The first layer included eight equidistant metallic rods in direct contact to the marble. Above these rods four wide flange H beams (HEB 140) were placed. The second layer consisted of four equidistant rods and two wide flange H beams (HEB 200). The beam of the last layer was supported on the previous layer through two metallic rods and it was loaded with the aid of another rod, in contact to the frame's traverse. Eight Linear Variable Differential Transformers (LVDTs) were used to measure deflections and two clip gauges were used to measure the relative displacement of two knife-edges attached on the fault's either side. The overall specimen's deformation was also monitored with the aid of innovative sensing techniques gaining data from suitable sensors, mounted on the specimen's surface. A proper arrangement of sensors of various types was designed, aiming to the most efficient pumping of data both from the external surface and the interior of the epistyle: Eight acoustic sensors were attached around the fault's area for the spatiotemporal determination of the location of sources of Acoustic Emissions and four electric contacts which permitted recording of the Pressure Stimulated Currents. In addition, the three dimensional displacement field of the epistyle's area in the immediate vicinity of the fracture plane was recorded using the Digital Image Correlation (DIC) technique. DIC is a full-field image analysis method, based on a sequence of digital images, which permits the determination of the contour and the displacements of mechanically loaded bodies. The epistyle was loaded monotonically under displacement-control mode at a rate ensuring quasi-static loading conditions. A general view of the overall experimental set-up and the sensors attached is shown in Fig.2. Further details, concerning the exact position of each sensor, the position of the reinforcing bars, the dimensions of the epistyle's copy and the loading scheme can be found in ref. [11, 12].



Figure 2: An overview of the experimental arrangement.

The Acoustic Emissions (AE) technique

When a rigid body is under mechanical loading and the stress field developed exceeds certain limits (depending on the body's material) elastic waves are emitted due to the nucleation of free surfaces and the subsequent release of stored elastic strain energy. These waves can be detected by proper acoustic sensors suitably attached on the material's surface. Monitoring AE provides useful information related to the spatiotemporal evolution of internal damage. Proper analysis of AE data is useful, among others, for the prediction of upcoming failure since they are strongly correlated with crack initiation and propagation [13]. The characteristics of the acoustic events recorded differ, in accordance to the nature of the sources of the events. It is nowadays accepted that, the signals caused by cracking are "explosive" with low duration while, on the other hand, signals related to shear phenomena (for example friction) are characterized by higher duration [13, 14]. In concrete, the classification of the type of cracks is standardized and implemented using the combination of the

average frequency of the pulse recorded by the sensors and a parameter called RA, which is in fact the ratio of the rise time (i.e., the time required for the pulse to reach its maximum value) over the maximum amplitude of the pulse. Signals of high frequency and low RA parameter are attributed to tensile cracks while signals of low frequency and high RA parameter are attributed to either shear- or mixed-mode cracks [15-17].

Another approach widely used to evaluate AE signals is the so called *b*-value analysis [21, 22]. Conventionally, the *b*-value analysis is based on the Gutenberg-Richter relationship, which is used in seismology and correlates events of high amplitude and lower frequency with events of low amplitude and higher frequency. Due to the fact that the determination of *b*-value is somehow subjective, an “Improved *b*-value” (*Ib*-value) was proposed in 1994 by Shiotani et al. [23, 24]. The *Ib*-value uses statistical parameters, as it is the mean and standard deviation of AE amplitude, which vary during the test. It is considered that increased *Ib*-values indicate that the system approaches a “critical stage”, or in other words failure is impending. The *Ib*-value is defined as:

$$I_b = \frac{\log_{10} N(\omega_1) - \log_{10} N(\omega_2)}{(\alpha_1 + \alpha_2)\sigma} \quad (1)$$

with $\omega_1 = \mu - a_1\sigma$, $\omega_2 = \mu + a_2\sigma$, where σ is the standard deviation, μ is the mean value of the amplitude distribution, a_1 is a coefficient related to the smaller amplitude and a_2 is a coefficient related to the fracture level. The values of a_1 and a_2 vary in the range 0.5-5.0, however it is proven that changing their value within the specific range does not significantly affect the *Ib*-value [23, 24]. In this context in the protocol described here it was considered that $a_1 = a_2 = 1.0$.

The Pressure Stimulated Currents (PSC) technique

The PSC technique is based on the detection of weak electrical signals emitted during the formation and growth of micro cracks within the material's bulk. The PSC technique has been applied on several materials (marble, amphibolite, cement based materials etc) [25-28] and under several mechanical loading types and so far it is proven that (at least in the laboratory scale) it provides consistent pre-failure indicators. According to the fundamental principles of the technique, the electric charge produced while a material is subjected to an external mechanical load is attributed to several reasons such as moving charged dislocations, the piezoelectric effect and the fracto-emissions.

The dislocations are a type of defect in crystals. The dislocations (point, linear, planar, bulk) are areas where the atoms are out of position in the crystal structure and move when a stress field is applied. They are not symmetric with respect to positive and negative charge and when deformation occurs, the dislocations start moving transporting charge. Piezoelectric effect is the ability of certain materials to generate electric charge in response to externally applied mechanical stress. In piezoelectric crystals, the unit cell is not symmetrical. Normally, piezoelectric crystals are electrically neutral, the atoms inside them may not be symmetrically arranged, but their electrical charges are perfectly balanced. The deformation of a piezoelectric material leads to push some of the atoms closer together or further apart, upsetting the balance of positive and negative, and causing net electrical charges to appear. Fracto-emission is the emission of particles (e.g., electrons, ions, ground state and excited neutrals, and photons) during and following fracture. The origin of electron and photon emission from fracture has frequently been attributed to either (a) field emission due to electric fields produced by charge separation or to (b) various non adiabatic processes involving fundamental excitations of creation and recombination of point like defects and charge carriers. Dickinson et al. [29] proposed a simple model for systems involving charge separation during fracture already since 1983.

EXPERIMENTAL RESULTS

The overall mechanical response of the restored epistyle

The load-deflection curve, plotted in Fig.3a, exhibits five distinct characteristic regimes, which do not appear in case an intact marble epistyle is subjected to bending [19, 20]. For almost three quarters of the maximum load imposed (i.e. the load that caused catastrophic failure and which was equal to about 375 kN) the epistyle behaves as an intact structure (portion OA of the graph in Fig.3a) and its response is almost perfectly linear, although the overall “stiffness” is well below of that characterizing intact Dionysos marble under bending [20]. It will be indicated later (by taking advantage of data provided by the Acoustic Emissions technique), that point A corresponds (quite possibly) to the time instant at which fracture of the cement layer between the marble fragments starts.

The linear portion of the graph is followed by a non-linear response of the restored epistyle (portion AB of the graph), which is in turn followed by a “plateau” BC. The specific behaviour appears similar to that of ductile metallic elements, (like

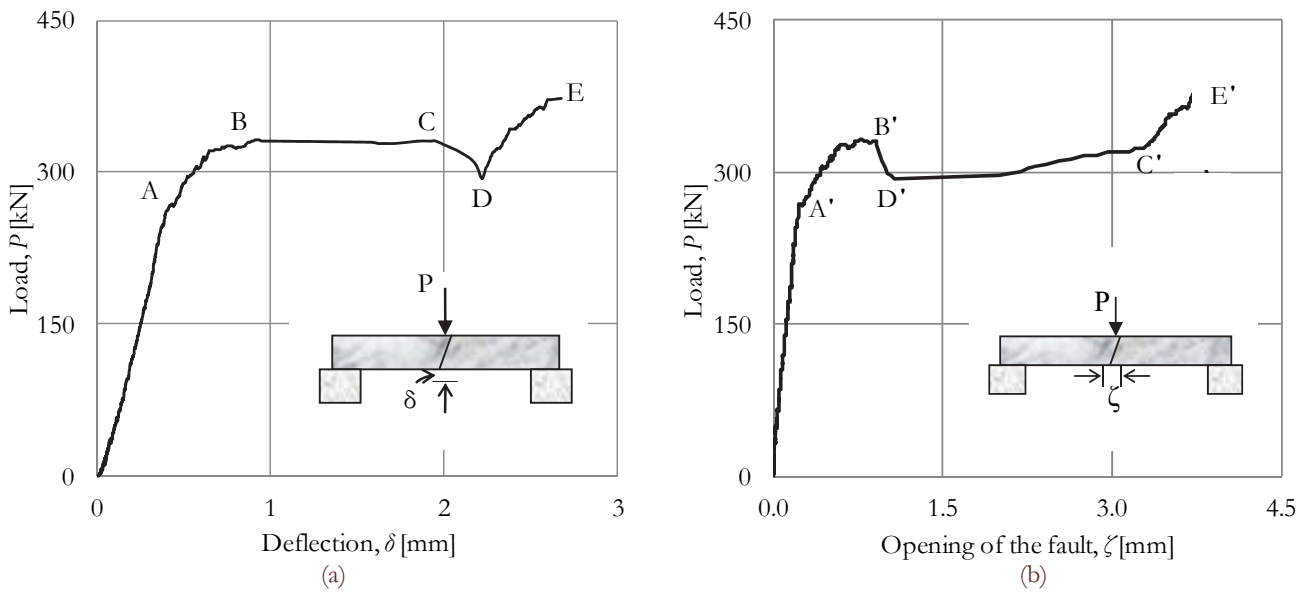


Figure 3: The overall load imposed versus the (a) deflection, δ , of the epistyle's central section and (b) the opening of the fault, ζ , at the lowest edge of the epistyle.

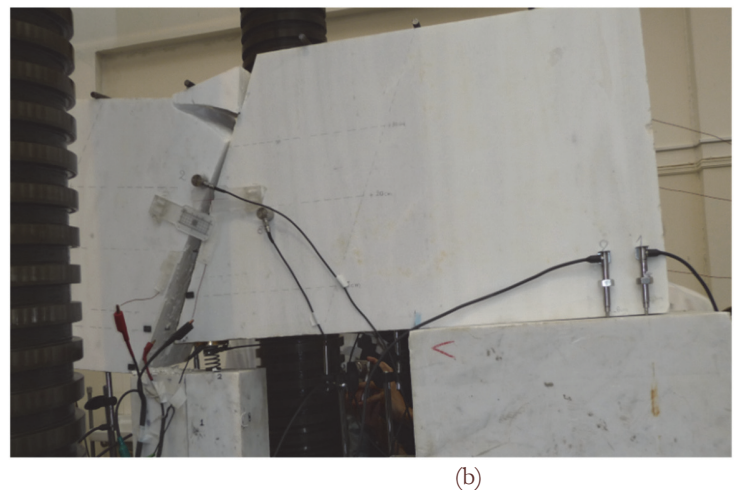
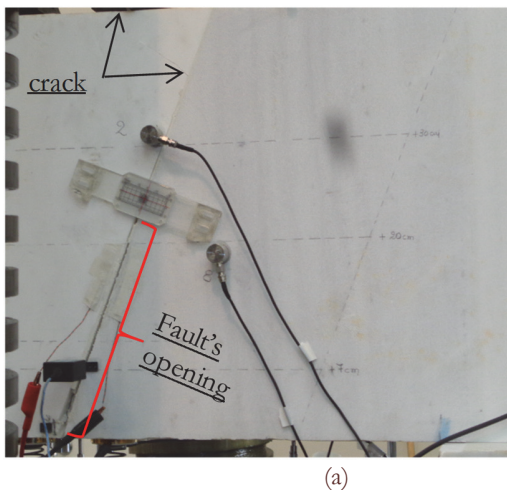


Figure 4: (a) First macroscopically visible cracking of the upper corner of the left fragment at time instant $t \sim 1140$ s. (b) The epistyle after the final failure (fracture of all reinforcing titanium bars).

titanium) under tension indicating, perhaps, some kind of yield and flow of the lowest level of reinforcing bars. The abrupt load drop following (portion CD of the graph) is difficult to be explained, however it could be attributed to either a local fracture of the upper corner of one of the two fragments (which is clearly seen in Fig.4) or to fracture of the titanium bars of the lowest layer or even to both of them. After this sudden drop the load starts increasing again, indicating that the additional load imposed is undertaken by the bars of the upper level, for which the stress level is below the respective yield limit. The maximum deflection recorded (at the maximum load imposed) was equal to about 2.7 mm.

The second mechanical parameter, of crucial importance, from the engineering point of view, is the opening, ζ , of the fault, i.e. the increase of the distance between the two fragments, which was measured with the aid of traditional clip-gauges attached at the lowest edge of the epistyle and also at the level of the lowest layer of restoring bars.

The variation of ζ versus the overall load imposed is plotted in Fig.3b. It exhibits a behaviour quite similar (from a qualitative point of view) with that of the deflection (Fig.3a). Again the dependence is initially linear, followed by a regime of non-linear response. However, instead of a "plateau" (as it was the case of the P - δ graph) the non-linear portion is terminated by a sudden drop and the characteristic "plateau" appears afterwards. Then the opening of the fault starts increasing again slowly until a value equal to about $\zeta = 3.2$ mm. From this point on, the increase becomes steeper attaining a

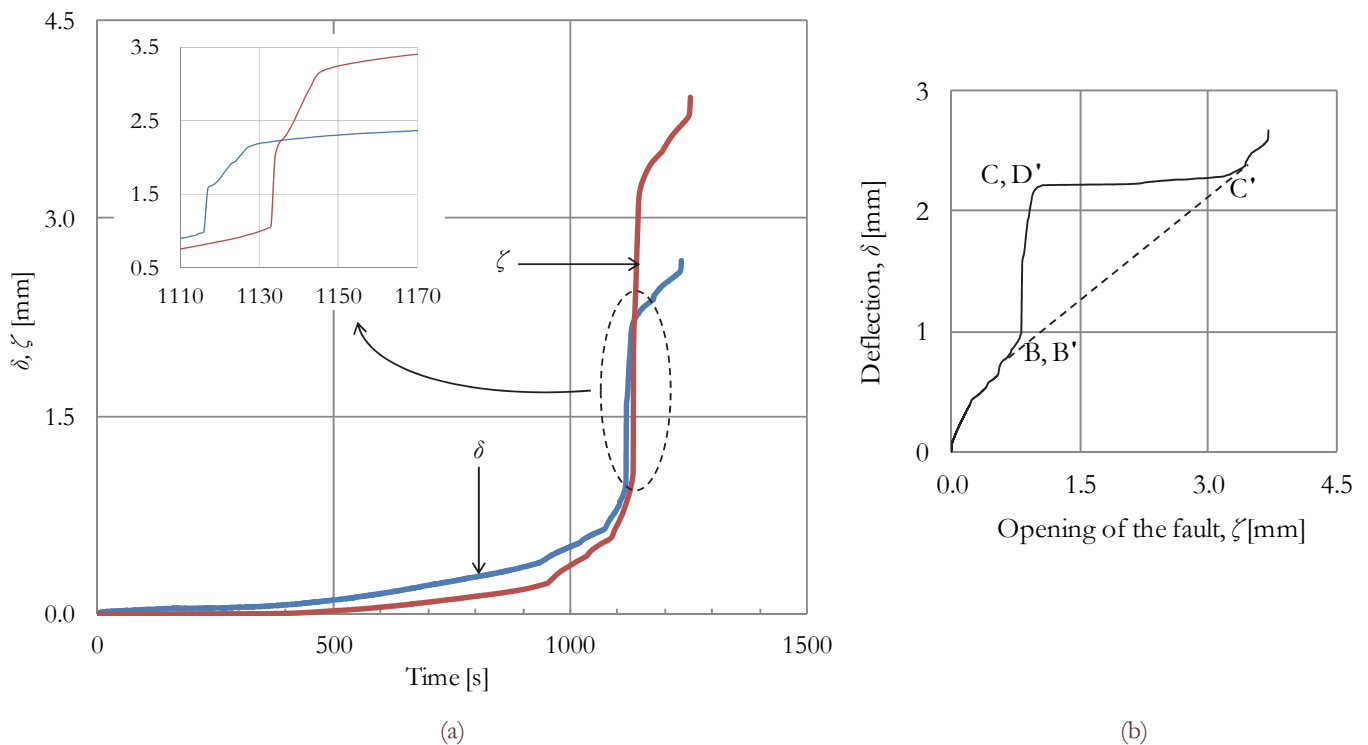


Figure 5: (a) The time evolution of deflection, δ , of the epistyle's central section and of the opening of the fault, ζ , at the lowest edge of the epistyle. (b) The dependence of δ on ζ .

maximum value equal to about $\zeta=3.5$ mm. The letters designating these characteristic intervals in Fig.3b are in accordance to those of Fig.3a. Attention should be paid, however, to the fact that their succession is not identical.

In order to follow the time evolution of δ and ζ , the time dependence of them is plotted in Fig.5a. The similarity of the two graphs is quite interesting. Both quantities exhibit an almost perfectly linear portion, followed by a non-linear one which is terminated by a characteristic “plateau” until about $t=1130$ s and then the deformation (either in terms of δ or ζ) starts increasing quite abruptly. From Fig.5a it could be concluded that the two “plateaus” do not appear simultaneously. As it is more clearly seen in the plot embedded in Fig.5a, a time shift between them appears. In the authors' opinion this should be attributed to differences in the sampling rate between the devices recording deflection (LVDTs) and those recording the fault's opening (clip-gauges) as well as to inevitable time-delays. This opinion can be supported by Fig.5b where δ and ζ are plotted against each other. It is reasonable to assume that neither δ can increase with ζ remaining constant (portion BC of the graph) nor can ζ increase with δ remaining constant (portion D'C'). Given that the number of experimental points between (B, B') and C' is very small it could be perhaps more wise to ignore the BCC' (or B'D'C') path and consider a virtual linear segment BC' instead.

In spite of the above discussed criticism, it is to be emphasized that, in general, the data provided by the clip-gauges for the opening of the fault are quite reliable. This was verified since they were found in excellent agreement with the respective data obtained from the Digital Image Correlation technique [32, 33]. The displacement field of both fragments was monitored by the cameras of the system during the whole duration of the loading procedure [11, 12]. A typical view of the epistyle as it is seen by the two cameras is shown in Figs.6(a,b). The specific images correspond to the very last loading steps. As a next step the axial (horizontal) component of the displacement vector was determined for both fragments. Typical colour-scale images of the axial displacement of the two fragments are exhibited in Figs.6(c,d,e) for three characteristic time instants. Fig.6c corresponds to a very early loading stage ($t=10$ s), Fig.6d corresponds to the load-level at which separation of the fragments starts ($t=405$ s) and Fig.6e to a load level relatively close to the entrance to the “critical stage” of the loaded system ($t=1085$ s).

For the quantitative correlation of the data provided by the DIC and the clip-gauges, two pairs of elementary areas of the fragments on either side of the fault were isolated in the immediate vicinity of the clips and the distance between them was determined as a function of time. The data concerning the opening of the fault as obtained from the DIC system are plotted in Fig.6f, in juxtaposition to those of the clip-gauges. It can be seen that the agreement between DIC and clip-gauges is excellent and the differences recorded do not exceed 1% for the whole duration of the loading procedure.

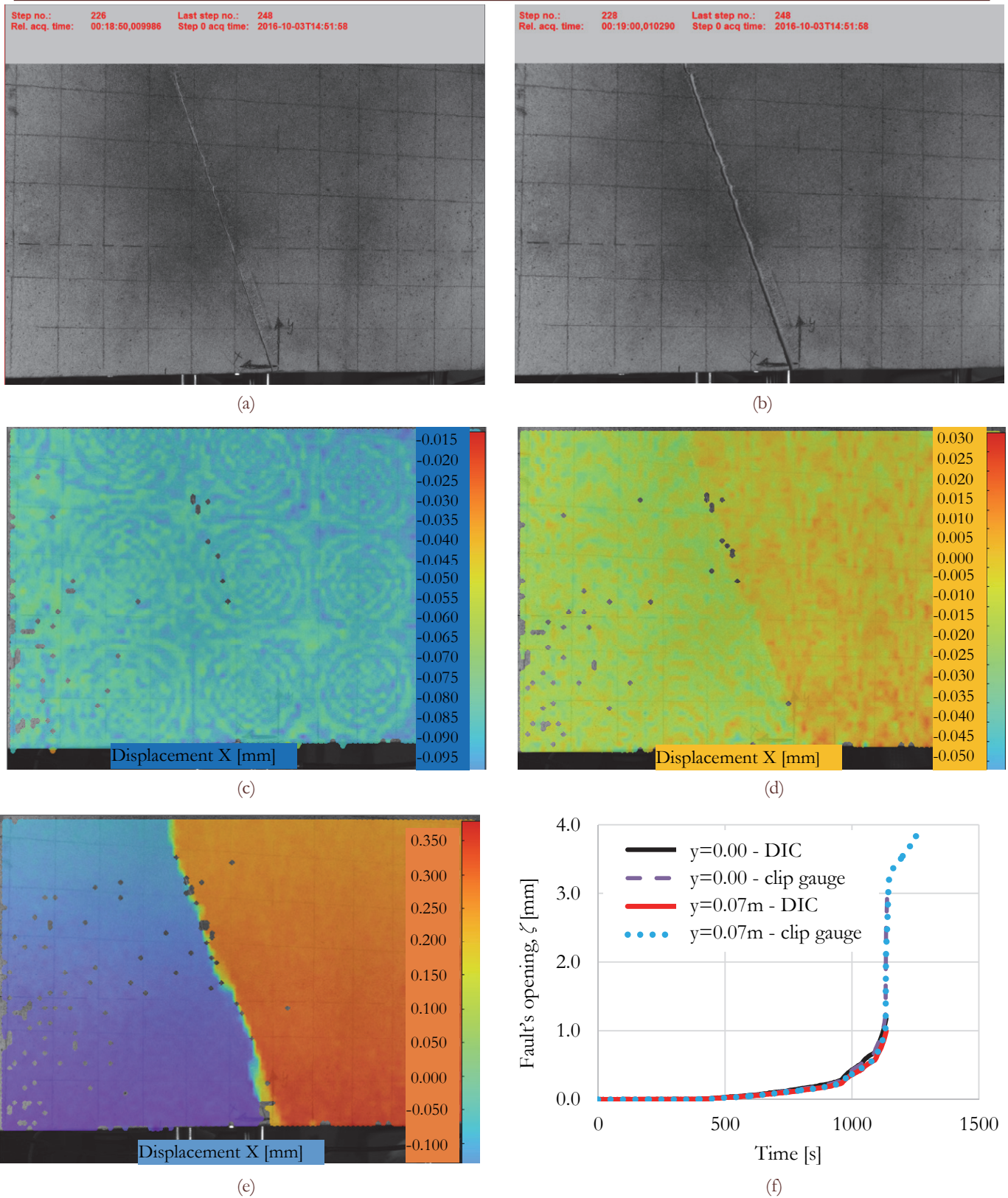


Figure 6: (a) (b) Typical view of the restored epistyle as it seen by the two cameras of the DIC system while failure is impending; (c) The contours of the axial displacement of the epistyle at time instants (c) $t=10s$; (d) $t=405s$; and (e) $t=1085s$; (f) The time variation of the opening of the fault as extracted by the DIC system and by the two clip gauges.

Concerning the overall response of the restored epistyle it was concluded by the data of the DIC system that (in excellent agreement with the conclusions drawn by the data of the remaining systems that will be analyzed in next sections) the epistyle behaves as an intact structure up to about $t=400$ s. Then the fragments start separating from each other and their distance increases relatively smoothly. Then at a time instant equal to about $t=1100$ s the separation tendency is accelerated denoting entrance of the system to its “critical stage” which will lead the structure to final collapse.

Data provided by the Acoustic Emission and the Pressure Stimulated Currents techniques

The variation of the PSC recordings against the opening of the fault is plotted in Fig.7 in juxtaposition to the respective variation of the load imposed. It is observed from this figure that the electric current produced during loading follows, according to a quite satisfactory manner, the respective variation of the load imposed. The PSC increases almost linearly during the very first steps of the loading procedure and then it is almost stabilized in the period of non-linear mechanical response of the restored epistyle. At the time instant of the sudden load drop the PSC starts increasing smoothly attaining a maximum value equal to about 2 nA. After this maximum its value starts decreasing more or less smoothly. A sudden drop is observed when the load level is equal to about 320 kN, i.e., the load level at which the crack opening starts increasing (see Fig.3b) designating approach to the final “critical stage” of the structure.

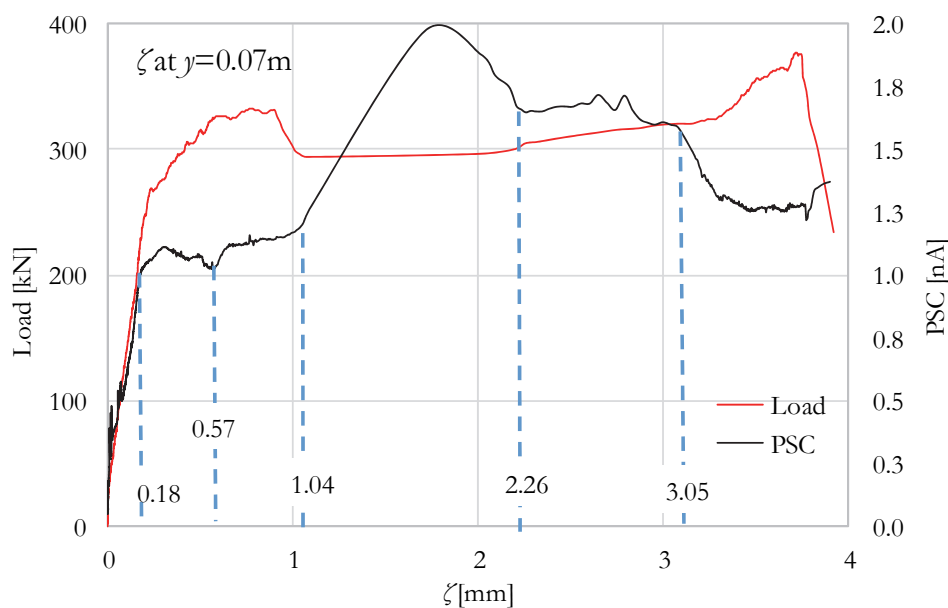


Figure 7: The variation of the load and the PSC versus the opening, ζ , of the fault.

It is quite interesting to note that the variation of PSC against the opening of the fault exhibits characteristic slope changes at points where the respective load-opening of the fault graph exhibits similar changes. These points, indicated by blue lines in Fig.7, are detected for values of the fault’s opening equal to $\zeta=0.18, 0.57, 1.04, 2.26$ and 3.05 mm. According to the previous discussion the first increasing part of the PSC graph (i.e., that until $\zeta=0.18$) can be attributed to the fracturing of the cement paste between the two fragments, the second one (i.e., that from $\zeta=1.04$) to cracking of the cement-paste surrounding the bars, while the last one (i.e., that after $\zeta=3.05$ mm) corresponds to the entrance of the “system” (restored epistyle) in its “critical stage” (i.e., the epistyle approaches its catastrophic failure) and can be safely considered as a relatively early “pre-failure” indicator. In general, the two phases of PSC increase (i.e., from $\zeta=0$ to $\zeta=0.18$ mm and from $\zeta=1.04$ mm to $\zeta=2.26$ mm) can be attributed to production of electric charge due to micro-cracking in the cement paste (and perhaps in the marble’s body), while the drops of its value are attributed to the appearance of cracks of larger size which interrupt conductive paths.

As a next step, in the direction of gaining an overview of the acoustic activity within the structure, the time rate of cumulative hits is plotted against time in Fig.8. In the same figure the time variation of the deflection, δ , and that of the fault’s opening, ζ , is also plotted for comparison. It is quite encouraging to observe that the time variation of the cumulative hits per second is quite similar (from a qualitative point of view) to the respective one of the PSC: It exhibits, also, characteristics slope changes at exactly the same time instants (or equivalently at the same values of the fault’s opening) as it was observed for the PSC. These changes are indicated by dotted lines in Fig.8, together with the respective values of the fault’s opening (mm).

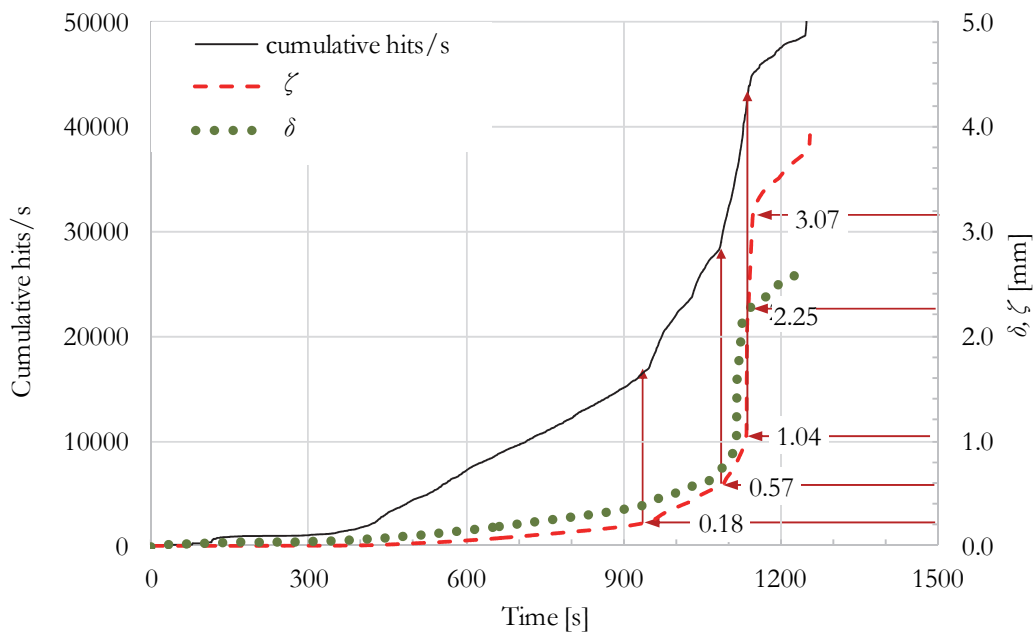


Figure 8: The time dependence of the cumulative hits per second in conjunction to that of the deflection and the opening of the fault.

An alternative approach of quantifying the acoustic activity within the restored epistyle is attempted in Fig. 9a: The cumulative energy of the acoustic emissions is plotted against the level of the mechanical load imposed to the structure in juxtaposition to that of the deflection, δ , of the epistyle's central section. The two plots exhibit the same qualitative characteristics: A stage of more or less smooth increase followed by a "plateau", a sudden change at the instant of the first load drop and again a stage of increase. The correlation of the cumulative energy of the acoustic emissions with the PSC is shown in Fig.9b, in which the dependence of both quantities on the load level is plotted. Besides partial differences it is evident that the overall behaviour of the two plots is quite similar to each other.

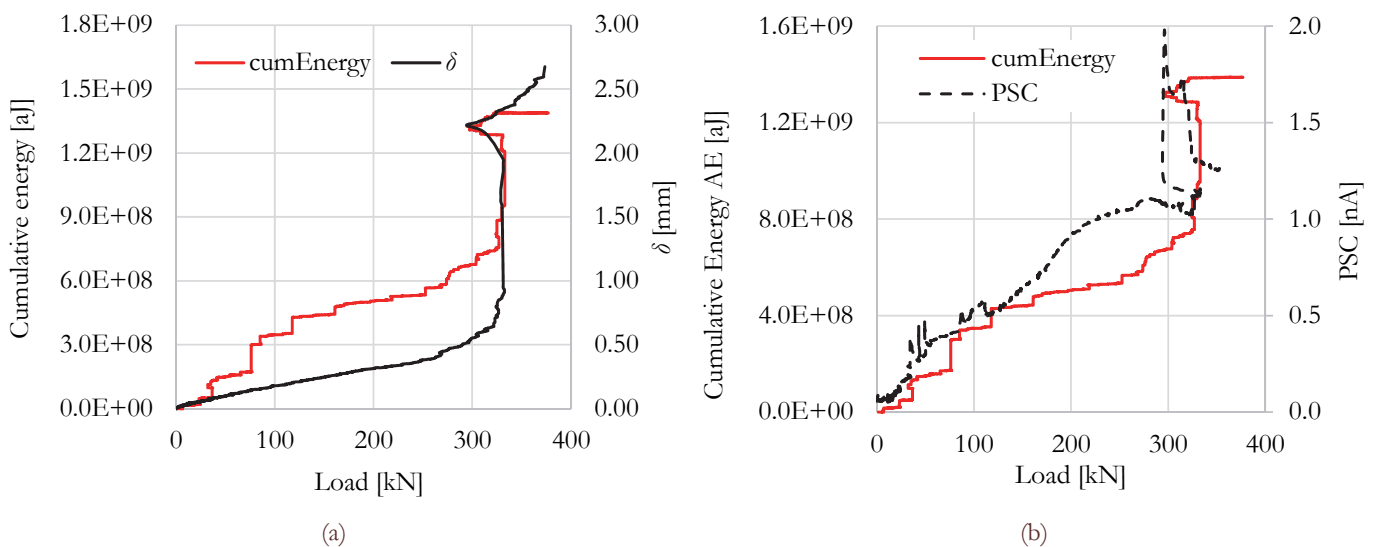


Figure 9: (a) The variation of the cumulative energy of the AE and δ versus the load applied; (b) The variation of the cumulative energy of the AE and PSC recordings versus the load applied.

Further exploitation of the experimental data provided by the acoustic sensors is achieved by calculating the respective Ib -value. In Fig.10 the time variation of the Ib -value is plotted in juxtaposition to the respective one of the load imposed. It is very interesting to observe that the Ib -value remains almost constant, equal to about $Ib=1.5$ for over 90% of the experiment's overall duration. At $t=1150$ s a decrease of the Ib -value is observed almost simultaneously with the abrupt

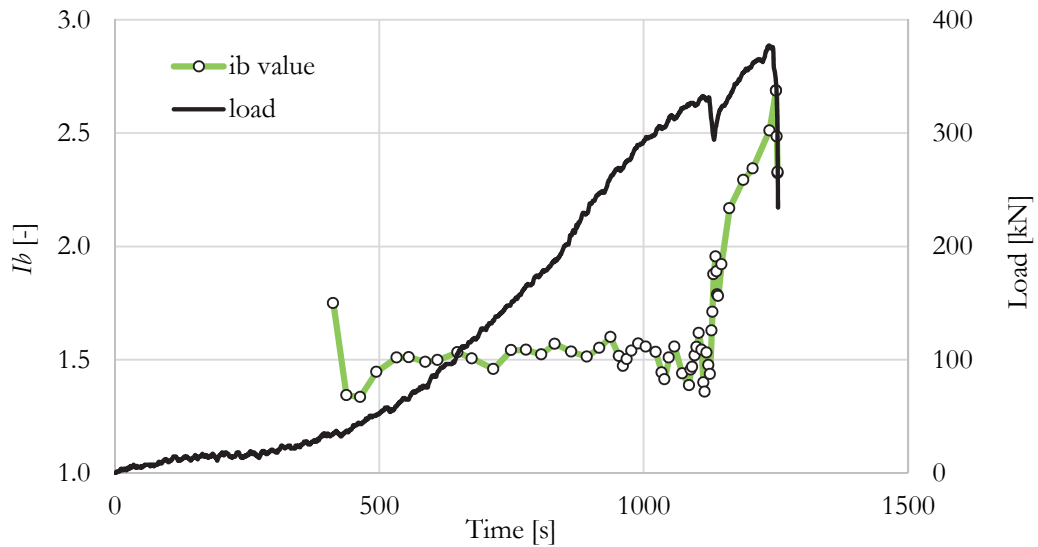


Figure 10: Time variation of the Ib -value in juxtaposition to the respective variation of the load imposed

load drop caused by the local fracture of the upper corner of one of the two fragments (Fig.4), which results, in fact, to an instantaneous relief of the stress field within the epistyle's body. After this time instant the load starts increasing again and the Ib -value increases abruptly reaching finally values even exceeding $Ib=2.5$. Similar behaviour of the Ib -value has been already observed and discussed in refs.[34, 35].

At the time instant at which the Ib -value starts increasing again after its drop at $t=1150$ s, a similar behaviour is exhibited by the RA parameter. This is clearly seen in Fig.11a, in which the time variation of RA is plotted in juxtaposition to that of the Ib -value: RA is very low, varying in the region $0 < RA < 5 \times 10^3 \mu s/V$ for the time-interval from $0 < t < 1150$ s. Suddenly at $t=1150$ s the value of RA is skyrocketed exceeding $20 \times 10^3 \mu s/V$, i.e., more than four times higher.

Along the same lines the time variation of the Ib -value is considered in comparison to the respective variation of the energy of the PSC [36]. The two plots are shown in Fig.11b. It is revealed from this figure that the energy of the PSC increases more or less smoothly against time for the time interval $0 < t < 1000$ reaching a maximum value equal to about $0.45 \text{ aA}^2\text{s}$. Then it remains almost constant until $t=1150$ s where it exhibits an explosive increase to a value exceeding $2.50 \text{ aA}^2\text{s}$, i.e., almost five times higher compared to the maximum value attained until the specific time instant. The specific conclusion is of utmost importance since it indicates again a close qualitative correlation between the recordings of the AE and PSC techniques, which could be used in the near future in the direction of quantitatively calibrating the PSC technique as Continuous Structural Healthy Monitoring tool.

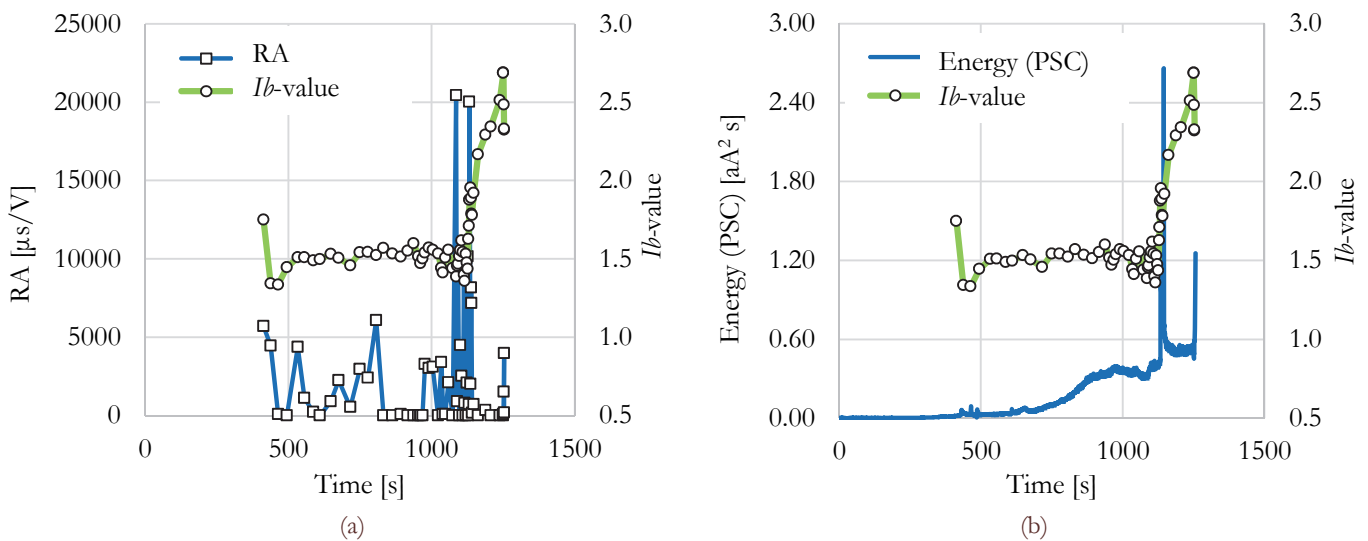


Figure 11: Time variation of the Ib -value in juxtaposition to the respective variation of (a) the RA parameter and (b) PSC energy.



THE SUCCESSION OF FAILURE MECHANISMS

In an effort to enlighten the failure mechanisms activated during the loading process of the restored epistyle the approach of considering the relation between the average frequency of the acoustic signals and their RA (rise time per amplitude) parameter, is adopted [16, 17]. The whole duration of the experiment was divided into four intervals according to the time evolution of hits/s which is shown in Fig.12. It is observed that during the first interval the number of hits per second is very small indicating negligible acoustic activity. During the second interval their number is considerably higher (exceeding fifty hits per second) with a smooth increasing tendency. During the third interval the number of hits per second attains huge values even exceeding three hundreds. Finally at the last interval the acoustic activity is again very low. It is worth mentioning that these intervals correspond with good accuracy to the time instants at which the plots of both the deflection and the opening of the fault against time exhibit characteristic slope changes, mentioned in previous sections. The average frequency of the acoustic signals is plotted versus RA in Fig.13a for the as above four time-intervals.

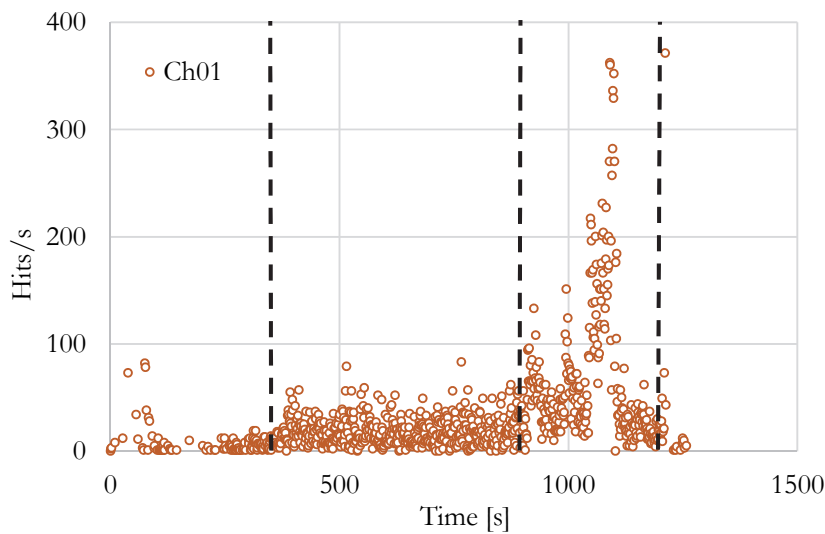


Figure 12: The time variation of the hits/s and the time intervals considered

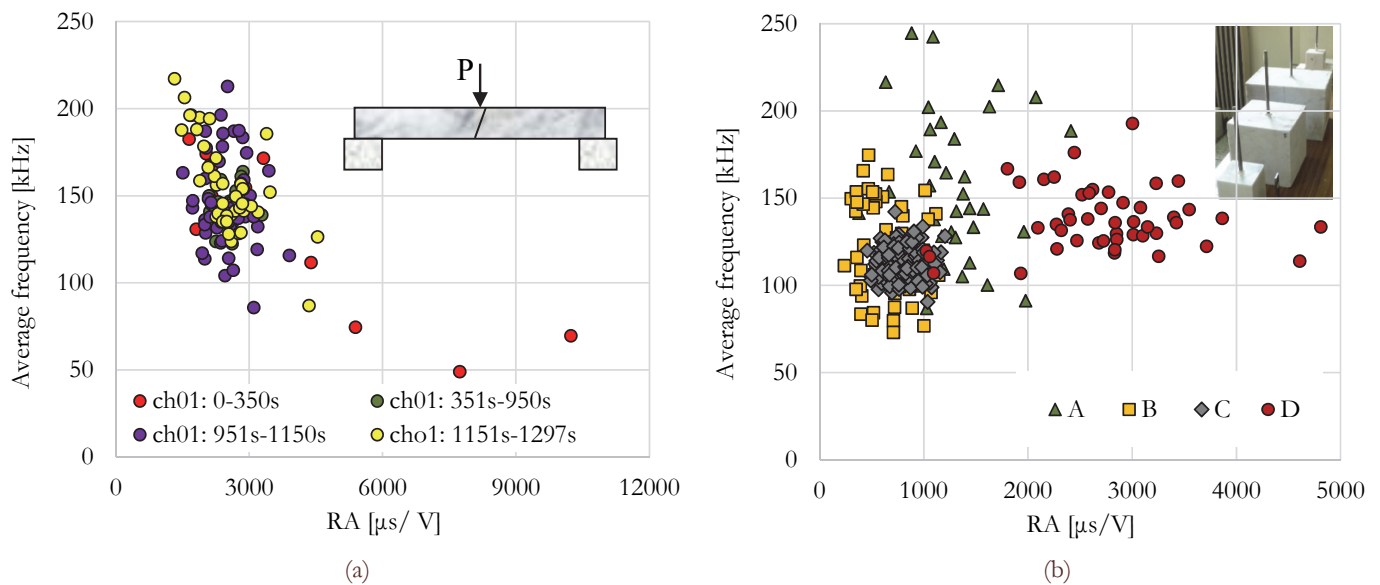


Figure 13: (a) The variation of the average frequency of the acoustic signals against the respective RA for the four time intervals considered; (b) The variation of the average frequency of the acoustic signals against the respective RA for a typical pull-out test [11], for four time intervals (A is the first and D the last one) [11].

It is clearly observed from Fig.13a that there are not striking differences between the signals for the four time intervals considered. Excluding very few signals of the first interval with relatively low frequency and increased RA-value, which could indicate preliminary shear (friction) effects (perhaps of parasitic nature), the vast majority of signals recorded are characterized by a combination of high frequency and low RA-value. It is therefore safely concluded that the specific design of the epistyle's restoration suppressed completely the pull-out phenomenon, i.e., the gradual removal of the reinforcing bars from the marble's body without fracture of neither the marble nor of the reinforcing bars. This is very interesting since the specific failure mechanism seriously concerns the members of the scientific personnel working for the restoration of the Acropolis monuments [37, 38]. Indeed, it has been verified both in the laboratory and also in the worksite that the weak link of the three-material complex (marble-cement paste-titanium) is the interface between the marble and the cement paste which due to pure adhesion fails prematurely [8-10]. It is mentioned, however, that the specific failure mechanism is not always "unwelcome", since it may act as a protective mean against failure (fracture) of the authentic marble body itself.

Further analysis of Fig.13a leads to the conclusion that during all four time-intervals the predominant failure mechanism is cracking due to normal stresses. In combination to the data of all sensing techniques it is concluded that during the first time-interval the element suffering from cracking is the layer of cement paste between the two fragments at the lower half of the member (i.e. its portion under tension). In a second phase cracking of the layer of cement paste that fills the holes and surrounds the metallic bars appears in the immediate vicinity of the interface (recall that according to previous numerical studies it is only a small portion of the anchoring length - equal to a few cm - that undertakes the tensile force balancing the externally applied bending load [8-10]). During the remaining time-intervals the element suffering from cracking is the body of the two marble fragments. It is emphasized, however, that the intensity of this type of cracking is not constant during the whole duration of the last two time intervals. Obviously a "silent" period, i.e. a period of low acoustic activity appears during yielding of the lower layer of reinforcing bars, which is indeed observed in Fig.12 around a time instant equal to about $t=1130$ sec.

In an attempt to further enlighten the specific issue the respective data concerning the mutual dependence of the average frequency and the RA-parameter are plotted in Fig.13b, as they were obtained from a typical pull-out test of a threaded titanium bar from a marble block [11]. It is emphasized that the specimens of the specific test (see the figure embedded in Fig.13b) were prepared, also, by experienced technicians of the Parthenon worksite and the materials used (marble, bar and cement paste that fill the hole in which the bar is driven) were exactly the same with those used for the construction of the epistyle's copy tested here, in order for a direct comparison to be possible. As it can be seen from Fig.13b at the initial stages of the experiment the signals are characterized by high frequency and low RA-value, indicating cracking as predominant failure mode (of the intermediate cement paste layers). Gradually the signals change and during the final stage of the experiment they are characterized by lower frequency and considerably higher values of the RA parameter, indicating clearly that pull-out has started and the predominant failure mode is slip of the cement paste with respect to the marble's body. The specific conclusion was further supported by the data of other sensing techniques as it is described in ref.[11].

The as above conclusions are further verified by the spatial variation of the acoustic signals, plotted in Fig.14 [12]. It is observed that initially the events are detected along the fault (at its lower two thirds). For the specific load level it is obvious that neither the bars yield nor the marble is fractured. Therefore the specific events are due to cracking of the cement paste between the two fragments. Afterwards the events are localized in two areas and more specifically the ones where the bars of the two lower layers intersect the fault's plane. Again the load level does not support cracking of the marble body and therefore these events are safely attributed to cracking of the cement paste layer surrounding the reinforcing bars.

DISCUSSION AND CONCLUSIONS

An accurate copy of a typical epistyle of the Parthenon's Temple was fractured into two asymmetric fragments and it was restored with the aid of six titanium bars according to the technique developed by the scientists of the "Committee for the Conservation of the Acropolis Monuments". The epistyle was subjected to multi-point bending with the aid of a special metallic structure consisting of I-shaped beams and cylindrical bars. The aim of the study was to comparatively assess the efficiency of two modern sensing techniques ("Acoustic Emissions" and the "Pressure Stimulated Currents") as Continuous Structural Health Monitoring tools.

From the Strength of Materials point of view it was found that the response of the epistyle to bending load was almost linear for about three quarters of the maximum load attained. A characteristic plateau of the load-deflection curve can be

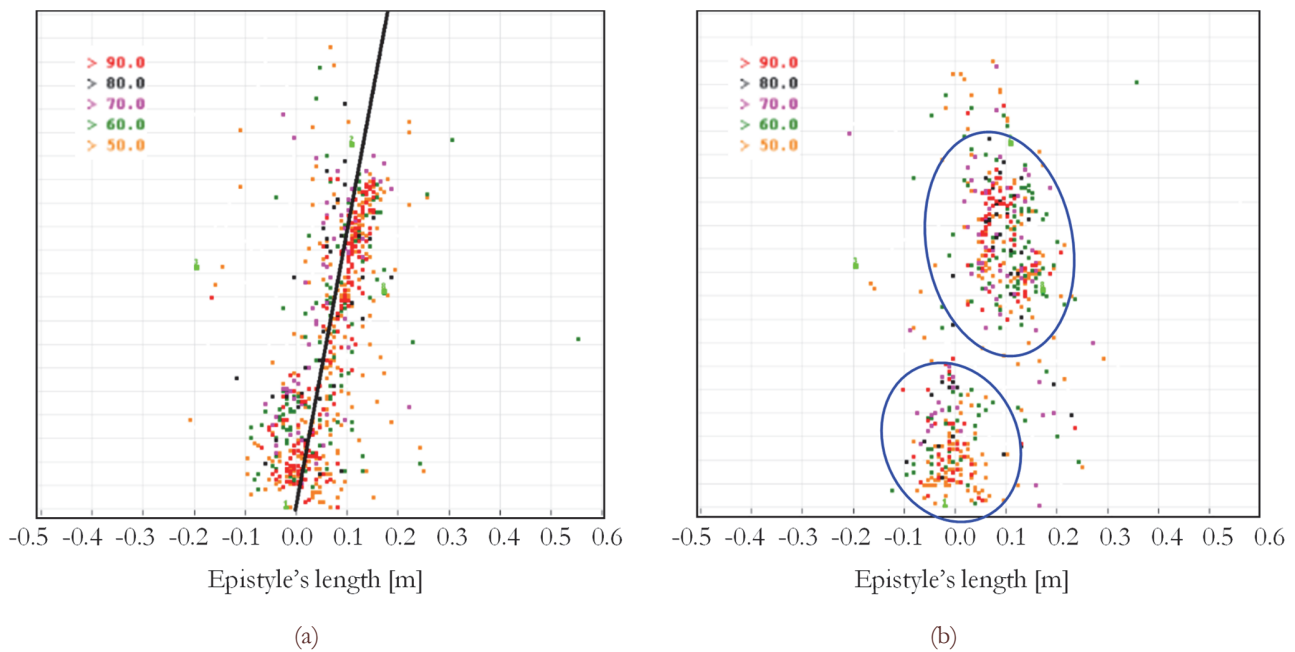


Figure 14: The spatial distribution of acoustic events for the second (a) and third (b) time intervals [12].

finally attributed to yielding of the reinforcing bars. The destruction of the restored structure (excluding a local fracture of a corner of one of the two fragments) appeared when the reinforcing bars of the lower layer yielded and fractured, triggering yielding and fracture also of the bars of the other two layers and causing collapse of the epistyle. The specific type of failure is not the worst scenario for scientists working for the restoration of monuments. Their worst scenario corresponds to fracture of the marble volumes. On the other hand, the failure mode here observed is not the most “desirable” one; the latter corresponds to the gradual pull-out of the reinforcing bars since (if timely detected) it permits undertaking of actions that can prevent final collapse. It could be therefore concluded that the pioneering technique developed and used for the restoration of monuments on the Acropolis of Athens should be further considered. What is to be answered is whether the procedure nowadays used to calculate the number of reinforcing bars and their diameter as well as the choice of the material they are made of are the most appropriate ones.

In addition, taking advantage of the data from all sensing techniques used, according to a combined manner, it was possible to clearly enlighten the succession of failure modes activated within the structure (which is a complex of three materials with two interfaces). It was definitely concluded that the final failure was the result of only two mechanisms: Cracking of the cement paste and marble (at different time intervals) and yielding and fracture of the reinforcing bars. The third failure mechanism, usually appearing in similar tests, i.e., the pull-out of the reinforcing bars, was totally suppressed.

Concerning the monitoring of the epistyle during loading it was concluded that all techniques used provided useful data of complementary nature. For example the data concerning the opening of the fault provided by the clip gauges were compared against the respective ones obtained by the Digital Image Correlation technique and were found in excellent qualitative and quantitative agreement. Therefore, depending on the needs and restrictions of specific experimental protocols either of them can be used. Along the same lines the data provided by the Acoustic Emissions and Pressure Stimulated Currents techniques were found in excellent qualitative agreement (recall that each technique is used to measure different quantities). The time variation of a series of parameters, quantified with the aid of these techniques (the electric current, the energy of the electric current, the cumulative hits per second, the cumulative energy of the acoustic events, the frequency of the signals and their RA-value, and the Ib-value), were found to exhibit characteristic changes (extreme values or slope changes) almost at identical time-instants. It is thus safe to conclude that the Acoustic Emission technique can be used to quantitatively calibrate the data of the Pressure Stimulated Currents and vice-versa, again depending on the needs of specific experimental protocols.

Of utmost importance is, also, the fact that both techniques (AE and PSC) provided clear signs which indicate entrance of the system to a “critical stage”, or in other words pre-failure indicators warning that final failure is impending. What is more it was concluded that various parameters could undertake the specific role: The electric current and the respective energy (concerning the PSC technique), the Ib-value, the cumulative number of hits, the RA value (concerning the AE technique). Obviously, the optimum choice (which could be a combination of more than one parameters) is something



that must be further studied in terms of data from additional experiments. In any case and beyond any doubt, both techniques were proven efficient tools for Structural Health Monitoring. The standardization of the respective procedure in practical field- applications related to the needs of Structural Health Monitoring of monumental structures (especially concerning the PSC technique which is up to now used only in laboratory level) seems to be the next challenging step. The advantages of the PSC technique, from the practical and aesthetical points of view (very small size of the sensors), and the relatively low cost of the respective sensors and monitoring tools, renders this effort quite reasonable.

REFERENCES

- [1] The restoration of the monuments of the Athenian Acropolis, 2nd ed., Ministry of culture and tourism-acropolis restoration service, dr. E. Lebidaki, Athens, (2011).
- [2] Angelides, S., Replacement of steel connectors by titanium alloy, The Acropolis: Problems-studies-measures to be taken, 2nd International Symposium on the Deterioration of Building Stones, Athens, Greece, (1976) 351-352.
- [3] Korres, M., Toganides, N., Zambas, C., Skoulikidis, Th., Study for the restoration of the Parthenon, Vol.2a, Ministry of Culture, Athens, Greece, (1989).
- [4] The Venice Charter, 1964. International charter for the conservation and restoration of monuments and sites, IInd International Congress of Architects and Technicians of Historic Monuments, Venice.
- [5] Acropolis Restoration Service, Principles and Methods. <http://www.ysma.gr/en/restoration-principles-and-methods>, 2011 (accessed 10/01/2017).
- [6] Kourkoulis, S.K., Ganniari-Papageorgiou, E., Bending of fragmented architraves restored with bolted titanium bars: A numerical analysis, *Engineering Transactions*, 56(2) (2008) 95-135.
- [7] Kourkoulis, S.K., Pasiou E., Epistyles connected with “P” connectors under pure shear, *Journal of the Serbian Society for Computational Mechanics*, 2(2) (2009) 81-99.
- [8] Kourkoulis, S.K., Mentzini, M., Ganniari-Papageorgiou, E., Experimental and numerical study of a fractured marble epistyle restored with layers of titanium bars, *The European Physical Journal Web of Conferences*, 6 (2010) 09002/1-09002/8.
- [9] Kourkoulis, S.K., Ganniari-Papageorgiou, E., Mentzini, M., Dionysos marble under bending: A contribution towards understanding the fracture of the Parthenon architraves, *Engineering Geology*, 115 (3-4) (2010) 246-256.
- [10] Kourkoulis, S.K., Mentzini, M., Ganniari-Papageorgiou, E., Restored marble epistyles under bending: A combined experimental and numerical study, *International Journal of Architectural Heritage*, 7(1) (2013) 89-115.
- [11] Dakanali, I., 2017. Applying innovative experimental techniques for the study of the mechanical behavior of structural members of ancient monuments and numerical simulation. PhD Thesis, Supervisor: Kourkoulis, S.K., National Technical University of Athens, Greece.
- [12] Kourkoulis, S.K., Dakanali, I., Monitoring the mechanical response of asymmetrically fractured marble epistyles after restoring their structural integrity, *Procedia Structural Integrity*, 3 (2017) 316-325.
- [13] Grosse, C.U., Ohtsu, M., Acoustic Emission testing, Basics for research - Applications in Civil Engineering, Springer-Verlag Berlin Heidelberg, (2008).
- [14] Miller, R.K., McIntyre, P., NDT handbook-acoustic emission testing, Columbus, OH: American Society for Nondestructive Testing, (1987).
- [15] Ohtsu, M., Recommendation of RILEM TC 212-ACD: acoustic emission and related NDE techniques for crack detection and damage evaluation in concrete, *Materials and Structures*, 43 (2010) 1187-1189.
- [16] Aggelis, D.G., Classification of cracking mode in concrete by acoustic emission parameters. *Mechanics Research Communications*, 38 (2011) 153-157.
- [17] Ohno, K., Ohtsu, M., Crack classification in concrete based on acoustic emission, *Construction and Building Materials*, 24 (2010) 2339-2346.
- [18] Kourkoulis, S.K., Exadaktylos G.E., Vardoulakis I., U-notched Dionysos-Pentelicon marble in three point bending: The effect of nonlinearity, anisotropy and microstructure, *International Journal of Fracture*, 98(3-4) (1999) 369-392.
- [19] Exadaktylos, G.E., Vardoulakis, I., Kourkoulis, S.K., Influence of nonlinearity and double elasticity on flexure of rock beams - I. Technical theory, *International Journal of Solids and Structures*, 38(22-23) (2001) 4091-4117.
- [20] Exadaktylos, G.E., Vardoulakis, I., Kourkoulis, S.K., Influence of nonlinearity and double elasticity on flexure of rock beams - II. Characterization of Dionysos marble, *International Journal of Solids and Structures*, 38(22-23) (2001) 4119-4145.



- [21] Gutenberg, B., Richter, C. F., In *Seismicity of the Earth and Associated Phenomena*, Princeton University Press, Princeton, NJ, USA, (1954) 2nd edn.
- [22] Rao M. V. M. S., Prasanna Lakshmi K. J., Analysis of b-value and improved b-value of acoustic emissions accompanying rock fracture, *Current Science*, 89 (9) (2005) 1577-1582.
- [23] Shiotani, T., Fujii, K., Aoki, T., Amou, K., Evaluation of progressive failure using AE sources and improved B-value on slope model tests. *Prog Acoust Emiss VII*, 7 (1994) 529–534.
- [24] Shiotani, T., Yuyama S., Li, Z. W., Ohtsu, M., Application of the AE improved b-value to qualitative evaluation of fracture process in concrete materials, *J. Acoust. Emission*, 19 (2001) 118–132.
- [25] Stavrakas, I., Triantis, D., Agioutantis, Z., Maurigiannakis, S., Saltas, V., Vallianatos, F., Pressure Stimulated Currents in rocks and their correlations with mechanical properties, *Natural Hazards and Earth System Sciences*, 4 (2004) 563-567.
- [26] Stavrakas, I., Anastasiadis, C., Triantis, D., Vallianatos, F., Piezo Stimulated currents in marble samples: Precursory and concurrent with failure signals, *Natural Hazards and Earth System Sciences*, 3 (2003) 243-247.
- [27] Triantis, D., Stavrakas, I., Anastasiadis, C., Kyriazopoulos, A., Vallianatos, F., An analysis of Pressure Stimulated Currents (PSC), in marble samples under mechanical stress, *Physics and Chemistry of the Earth*, 31 (2006) 234-239.
- [28] Triantis, D., Anastasiadis, C., Vallianatos, F., Kyriazis, P., Nover, G., Electric signal emissions during repeated abrupt uniaxial compressional stress steps in amphibolite from KTB drilling. *Natural Hazards and Earth System Sciences*, 7 (2007) 149-154.
- [29] Dickinson J.T., Jensen L.C., Jahan-Latibari A., Fracto-Emission: The Role of Charge Separation, *J. Vacuum Science Technology*, A2(2) (1983) 1112-1116.
- [30] Vardoulakis, I., Exadaktylos, G.E., Kourkoulis, S.K., Bending of marble with intrinsic length scales: A gradient theory with surface energy and size effects, *Journal de Physique IV*, 8 (1998) 399-406.
- [31] Kourkoulis, S.K., Stavropoulou, M.C., Vardoulakis, I., Exadaktylos, G.E., Local Strains Due to Punch Effect in Three Point Bending of Marble Beams, *Proceedings 9th Int. Congress on Rock Mechanics*, Paris, France, 25-28 August 1999, G. Vouille and P. Berest (eds.), A.A. Balkema, Rotterdam, The Netherlands, (1999) 623-626.
- [32] Sutton, MA., Cheng, M., Peters, WH., Chao, YJ., McNeill, SR., Application of an optimized digital correlation method to planar deformation analysis, *Image and Video Computing*, 4(3) (1986) 143-150.
- [33] McCormick, N., Lord, J., Digital Image Correlation, *Materials Today*, 13(12) (2010) 52-54.
- [34] Aggelis, D.G., Soulioti, D.V., Sapouridis, N., Barkouls, N.M., Paipetis, A.S., Matikas, T.E., Acoustic emission characterization of the fracture process in fibre reinforced concrete, *Construction and Building Materials*, 25 (2011) 4126-4131.
- [35] Kui, Z., Zhicheng, Z., Peng, Z., Sanjian, C., Experimental study on Acoustic Emission characteristics of Phyllite specimens under uniaxial compression, *Journal of Engineering Science and Technology Review*, 8(3) (2015) 53-60.
- [36] Triantis, D., Pasiou, E.D., Stavrakas I., Dakanali, I., Kourkoulis, S. K., Correlation of pressure stimulated currents and acoustic emissions during 3PB of cement-mortar beams and the role of loading rate, *Procedia Structural Integrity*, 3 (2017) 346–353.
- [37] Mentzini M., The bending of restored architrave: An evaluation, *Proc. 6th Int. Meeting for the Restoration of the Acropolis Monuments*, Chapter 4.3.2.1, 1-21, Hellenic Ministry of Culture and Sports, Committee for the Conservation of the Acropolis Monuments, Acropolis Museum Auditorium, Athens, October 4-5, 2013.
- [38] Toumbakari, E.-E., Analysis and interpretation of the structural failures of the orthostate in the northern wall of the Athens Parthenon, *Strain*, 45(1) (2009) 456–467.